

Vanadium Oxides on Aluminum Oxide Supports. 3. Metastable κ -Al₂O₃(001) Compared to α -Al₂O₃(0001)

Tanya K. Todorova, M. Veronica Ganduglia-Pirovano,* and Joachim Sauer

Humboldt-Universität zu Berlin, Institut für Chemie, Unter den Linden 6, D-10099 Berlin, Germany

Received: October 30, 2006; In Final Form: January 24, 2007

Low-coverage vanadia species (monomers, dimers, trimers, and one-dimensional vanadia rows) as well as vanadium oxide films of varying thickness supported on the metastable κ -Al₂O₃(001) surface are investigated by density functional theory in combination with statistical thermodynamics. At low-vanadium chemical potentials and typical reducing conditions, species with V–O⁽³⁾–Al interface bonds are stable. These aggregates are partially reduced with vanadium in the V^{III} oxidation state. This correlates with defect formation energy values for the initial removal of lattice oxygen in the range of 1.3–2.7 eV. As the length of the polymeric species increases, the reduction energy decreases. We demonstrate that the support structure does affect the structure of the model catalyst and the lattice oxygen bond strength. On the α -Al₂O₃(0001) surface, the only stable low-coverage VO_x species are dimers with V–O⁽²⁾–Al interface bonds and a defect formation energy of 2.8 eV. Reduction remains more facile for vanadia films on κ -Al₂O₃ than on α -Al₂O₃. The systematic lower values relate to the presence of tetrahedral sites that allow for significant lattice relaxation upon reduction. Using the oxygen defect formation energy as a reactivity descriptor, we discuss possible effects of the support structure and vanadia loading in Mars-van Krevelen-type oxidation reactions. We also analyze the influence of the support structure on the interface vibrational modes.

I. Introduction

Supported vanadium oxide catalysts have been studied extensively over the past two decades because of their potential to catalyze several important oxidation reactions (e.g., the oxidation of methanol to formaldehyde and the oxidative dehydrogenation of light alkanes).^{1–7} The catalysts consist of a vanadia phase deposited on the surface of an oxide support, such as SiO₂, Al₂O₃, TiO₂, and ZrO₂. It is known that the activity of the catalysts can be modified by up to several orders of magnitude by changing the support material.^{4,5,7} However, the origin of this support effect and the role of the vanadia/support interface on the reactivity of vanadia aggregates are not well understood. The reason is the complexity of the surface structure of the (real) supported catalysts under catalytic relevant conditions.

Recently, model catalysts consisting of vanadium oxide particles on an alumina support grown on NiAl(110) were experimentally examined under ultrahigh vacuum (UHV) conditions.^{8,9} Moreover, vanadia monolayers ($\sim 2\text{Å}$)¹⁰ and thicker films (up to $\sim 6\text{Å}$)¹¹ as well as small vanadia clusters (V₂O₅ and V₂O₄)¹² on an α -Al₂O₃ support were investigated using density functional theory (DFT). The α -Al₂O₃(0001) surface in these theoretical studies was chosen as support because of its simplicity, whereas the atomic structure of the alumina/NiAl(110) film was not known. The film has been characterized by various methods.^{13–18} Results from transmission electron microscopy and phonon spectra point to a γ -like Al₂O₃ structure.^{13,15,17} However, based on surface X-ray diffraction measurements a κ -like structure has been derived.¹⁹ Combining high-resolution scanning tunneling microscopy (STM) images and DFT calculations, the atomic structure of the thin alumina film

on NiAl(110) has been finally resolved.^{20,21} It differs from any known Al₂O₃ bulk phase and includes a mixture of tetrahedrally and pyramidally coordinated Al ions. All the metastable bulk phases (e.g., γ -, δ -, η -, θ -, χ -, and κ -alumina) have in common Al ions not only in octahedral (Al^O), as in α -Al₂O₃, but also in tetrahedral (Al^T) coordination.

In fact, the structure of the alumina support of most real vanadia catalysts is that of γ -Al₂O₃. A wide variety of models for the γ -phase have been proposed over the last half century, but no consensus has been reached on issues such as the arrangement of vacancies on aluminum sites and the role of hydrogen in the structure (see, e.g., refs 22–26). Additionally, γ -Al₂O₃ has a high degree of disorder and shows diffuse diffraction patterns with strong structural similarities with other transition aluminas. Therefore, as a step toward modeling more realistic alumina-supported vanadia catalysts, we investigate κ -Al₂O₃ as support material. It is the only metastable alumina phase with a well-defined atomic structure and a moderate fraction (25%) of occupied tetrahedral sites.²⁷ We study different low-coverage VO_x species as well as films of varying thickness on the κ -phase and make comparisons with the results obtained for vanadia aggregates supported on the stable α -Al₂O₃ phase. This allows for examining the effect of Al^T sites on the structure of the supported species. Statistical thermodynamics is applied to account for the effect of oxygen partial pressure and vanadium concentration at a given temperature on the stability of the supported vanadia aggregates. We aim at understanding how VO_x species anchor to the surface of these two structurally different aluminas. Moreover, we discuss the effect of the support structure on the formation of oxygen defects in the vanadia phase. Vanadia-catalyzed oxidation reactions are known to proceed via the Mars-van Krevelen mechanism in which the (rate-determining) oxidation of the reactant is decoupled from the reoxidation of the catalyst. In accord with this mechanism,

* To whom correspondence should be addressed. vgp@chemie.hu-berlin.de.

we use the formation energy of a single lattice oxygen defect as a reactivity descriptor in such oxidation reactions. Because little is known about the surface structure of supported metal oxides and vibrational spectroscopy is one of the major tools for structural characterization, we analyze the influence of the support structure on the interface vibrational modes.

II. Methods

The present spin-polarized calculations are based on DFT within the generalized gradient approximation (GGA) using the PW91 exchange-correlation functional.²⁸ Plane wave basis set with a kinetic energy cutoff of 250 eV is employed as implemented in the Vienna ab initio simulation package (VASP).^{29–31} The electron–ion interaction is described by the projector augmented wave (PAW) method.^{32,33} The positions of the ions are relaxed by a conjugate-gradient algorithm until the forces are smaller than 0.01 eV/Å. Surface slabs representing the κ -Al₂O₃(001) surface are separated by a vacuum region of 10 Å, and the integrations in the Brillouin zone employ a (4 × 2 × 1) Monkhorst–Pack grid.³⁴

The oxygen defect formation energies, E_f , are calculated as the difference between the defect formation energy with respect to the oxygen atom (calculated at a 250 eV cutoff) and half the dissociation energy of the O₂ molecule in the gas phase.³⁵ The latter has been obtained using a 400 eV cutoff and smaller radii for the s and p states of oxygen by 0.30 and 0.38 au, respectively. The accuracy of this approach is verified by test calculations performed entirely at a 400 eV cutoff, which have shown systematic changes in the defect formation energy of about 0.1 eV.³⁵ The calculated dissociation energy of O₂ is 6.29 eV, whereas the experimental value is 5.17 eV (obtained after adding the contributions due to zero-point vibrations).³⁶ A (13 × 14 × 15) Å³ orthorhombic unit cell with Γ -point sampling of the Brillouin zone is employed.

The vibrational spectra are calculated using the harmonic approximation within the finite difference method with 0.02 Å displacements. The intensities are obtained from the derivatives of the dipole moment component perpendicular to the surface.

III. Models

A. Bulk and (001) Surface of κ -Al₂O₃. κ -Al₂O₃ crystallizes in an orthorhombic structure within the space group $Pna2_1$. The optimized lattice constants of the bulk unit cell are: $a = 4.88$ Å, $b = 8.39$ Å, and $c = 9.02$ Å, which are in excellent agreement with the experimental lattice constants $a_{\text{exp}} = 4.84$ Å, $b_{\text{exp}} = 8.33$ Å, and $c_{\text{exp}} = 8.95$ Å,³⁷ as well as with previously reported DFT-GGA results.^{38,39} In the unit cell, 75% of the Al atoms are Al^O and 25% are Al^T coordinated, which leads to two different types of Al layers alternating along the [001] direction (see Figure 1). The first type (“octahedral”) is composed of Al^O ions only, whereas the second contains equal amount of Al^O and Al^T and is called a “mixed” layer. The presence of Al^T sites creates large holes in the octahedral Al layers making the structure much more open compared to that of the α -phase.

In contrast to α -Al₂O₃, κ -Al₂O₃ lacks mirror symmetry through the (001) plane, making the two (001) and (00 $\bar{1}$) surfaces inequivalent. As a consequence, the existence of a one-dimensional (1D) metallic surface state on κ -Al₂O₃(00 $\bar{1}$) has been predicted.³⁸ It has been recently suggested that it may have useful applications in carbon nanotubes fabrication because of its affinity to strongly interact and chemisorb graphite sheets.⁴⁰ Test calculations have shown that such metallic state would have a dramatic effect on the reducibility of the vanadia aggregates supported on the (001) surface of the slab. Therefore, we

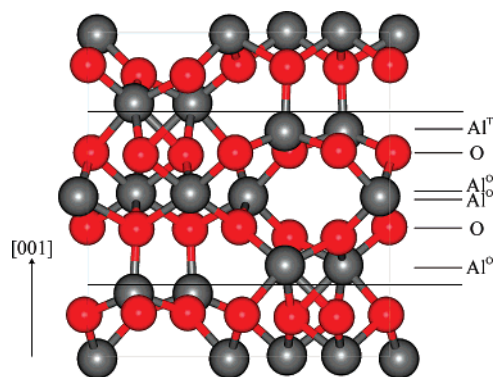


Figure 1. Bulk structure of κ -Al₂O₃. The stacking sequence of oxygen and aluminum layers along the [001] direction is shown. O and Al atoms are represented by red and dark gray spheres, respectively. One sixlayer with the following sequence of atomic layers Al₂^T–O₆–Al₂^O–Al₂^O–O₆–Al₂^O is indicated.

terminated the bottom (00 $\bar{1}$) surface by water molecules, thus “quenching” the metallic state and keeping the Al₂O₃ composition unchanged.

The atoms in the unit cell of κ -Al₂O₃ are stacked along the [001] direction in 16 planes of Al atoms and 8 planes of O atoms in a sequence Al₂^T–O₆–Al₂^O–Al₂^O–O₆–Al₂^O...–Al₂^T (see Figure 2). In the following, the term sixlayer is used for the repeating unit (Al₂^T–O₆–Al₂^O–Al₂^O–O₆–Al₂^O). The κ -Al₂O₃(001) surface is modeled by a slab consisting of four such sixlayers. It has a dipole moment perpendicular to the surface due to the non-symmetrical interlayer distances around the middle plane of each sixlayer. Thus, according to Tasker’s third rule the surface is polar.⁴¹ Actually, none of the conceivable terminations that can be obtained upon cleavage along the [001] direction is nonpolar and significant relaxations contribute to the surface stabilization.^{38,39} The unrelaxed κ -Al₂O₃(001) surface slab in our calculations is terminated by a single aluminum layer. A recent theoretical study on the metastable κ -Al₂O₃ revealed that this is the most stable surface termination.³⁹ It resembles the single metal termination of the corundum α -phase but has two outermost Al atoms per surface unit cell.

The relaxed κ -Al₂O₃(001) supercell was constructed in the following way. First, the coordinates of the two topmost sixlayers at the (001) surface were kept fixed at their bulk positions, while the bottom (001) surface was terminated with two H₂O molecules (one per surface Al ion) and the two bottom sixlayers were fully relaxed. Second, the optimized coordinates of the (001) surface were kept fixed and the (001) surface relaxed.

Table 1 lists the distances between the atomic planes of the topmost sixlayer of the κ -Al₂O₃(001) surface in the relaxed system compared to the ideal bulk-truncated structure. The atomic planes are denoted with superscripts (e.g., Al¹, O², Al³, Al⁴, O⁵, and Al⁶). The Al atoms of the topmost metal layer (Al¹) move inward by 153% or 0.90 Å (i.e., they move inside the holes of the octahedral Al layer). Similarly, the oxygen layer (O²) relaxes inward by 21% or 0.24 Å forming a buckled oxygen layer (see Figure 2). Thus, upon relaxation the clean κ -Al₂O₃(001) surface becomes oxygen-terminated and the outermost Al atoms recover their bulk tetrahedral coordination.

B. Low-Coverage VO_x Species and Vanadia Films Supported on κ -Al₂O₃(001). In the same way as in the previous studies of V_nO_m films on α -Al₂O₃,^{10,11} vanadium oxides supported on κ -Al₂O₃(001) can be modeled by subsequent replacing of Al by V atoms. Monomeric and polymeric species as well as vanadia films of varying thickness are thus created.

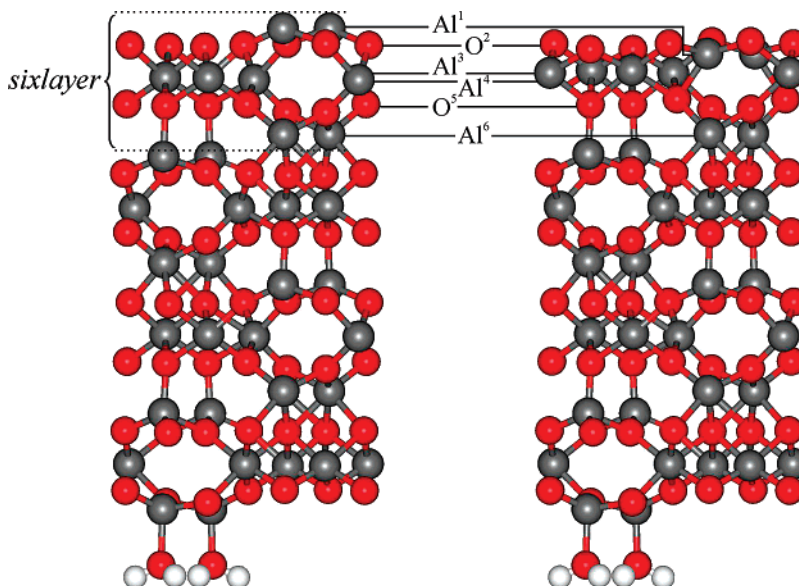


Figure 2. Structure of the clean κ -Al₂O₃(001) surface before and after relaxation (side view). The vertical lines indicate the stacking sequence of atomic layers along the z-direction. The repeating unit (sixlayer) is also marked. The (001) surface is terminated with H₂O molecules.

TABLE 1: Interlayer Spacing (Å) of the Ideal (Bulk) and Relaxed Structure of the Clean κ -Al₂O₃(001) Surface as Well as the Distance Difference Δz_{ij} ^a

	z_{ij} (bulk)	z_{ij} (relaxed)	Δz_{ij}
Al ¹ –O ²	0.59	0.31	–0.90
O ² –Al ³	1.13	0.89	–0.24
Al ³ –Al ⁴	0.09	0.09	±0.00
Al ⁴ –O ⁵	0.96	1.10	+0.14
O ⁵ –Al ⁶	0.95	1.03	+0.08

^a For the notation of the atomic layers, see Figure 2.

We define the surface vanadium coverage $\Theta = N/N_{\max}$, where N and N_{\max} are the actual and the maximum number of vanadium atoms per surface area A . Depending on the Θ values, we consider two types of supported vanadium oxides: low-coverage VO_x species ($\Theta \leq 1$ ML) and vanadia films ($\Theta > 1$ ML).

We have modeled different structures with $\Theta \leq 1$ ML, which are schematically shown in Figure 3, namely monomeric vanadia species at $\Theta = 0.25$ and 0.5 ML, dimers ($\Theta = 0.5$ ML), trimers ($\Theta = 0.75$ ML), and 1D vanadia zigzag rows along the [100] direction at $\Theta = 1$ ML. The isolated V sites at $\Theta = 0.25$ ML (Figure 3A) and $\Theta = 0.5$ ML (Figure 3B) are obtained by replacing one of the outermost Al atoms by V in the clean κ -Al₂O₃ surface with a (2 × 1) and (1 × 1) periodicity, respectively. Two neighboring V sites are separated by 9.77 and 4.88 Å, respectively. The dimeric ($\Theta = 0.5$ ML) and trimeric ($\Theta = 0.75$ ML) species are modeled in a (2 × 1) cell by replacing two and three out of the four topmost Al atoms by V, respectively (cf. Figure 3C,D). The dimer is a real dimer because the two V sites share an oxygen atom (V–O⁽³⁾–V bond). Further replacement of all topmost Al atoms results in a 1D vanadia row (Figure 3E). Formally, it is a 1V-layer film ($\Theta = 1$ ML), but the neighboring rows are not connected by V–O–V bonds. The dimers and trimers as well as the 1D vanadia rows are referred to as polymeric VO_x species. By adding oxygen atoms to the vanadium centers, vanadyl (O=V) sites are created. For all structures with the (2 × 1) periodicity, a (2 × 2 × 1) k -point grid is employed.

The coordination of the outermost Al atoms of the vanadyl-terminated low-coverage species varies with respect to that of the clean κ -Al₂O₃(001) surface (4-fold): monomers at $\Theta = 0.25$

ML and dimers ($\Theta = 0.5$ ML) have only one 5-fold coordinated Al atom, whereas for monomers at $\Theta = 0.5$ ML and trimers all surface Al atoms are 5-fold coordinated.

Moreover, vanadia films with (1 × 1) periodicity and coverage $\Theta > 1$ ML have been considered. The unit cell compositions have the general formula $(n/2)V_2O_5 \cdot ((32 - n)/2)Al_2O_3$ ($n = 4, 6, 8, \text{ and } 10$), whereas the composition of the fully vanadyl-terminated films is $(n/2)V_2O_5 \cdot ((32 - n)/2)Al_2O_3$, respectively. Figure 3 shows the O=V-covered vanadia films supported on the κ -Al₂O₃(001) surface with thicknesses of up to five vanadium layers. Similar to the V₂O₃(0001) surface⁴² as well as thick vanadia films supported on α -Al₂O₃(0001),¹¹ vanadia films supported on κ -Al₂O₃(001) surface may reconstruct. On the basis of the structure of 4V- and 5V-layer films, we built two models in which one or two of the surface vanadyl groups are removed and the vanadium atom(s) from the fourth V-layer pop into the hole of the outermost octahedral layer. The unit cell size, however, does not change.

C. Gas-Phase and Adsorbed V₂O₅ and V₂O₄ Clusters.

Linear and cyclic V₂O₅ and V₂O₄ gas-phase clusters are placed in a cubic box with $a = 15$ Å and the calculations were performed using the Γ -point only. The cyclic V₂O₅ structure is by 0.96 eV more stable than the linear one. The obtained geometries are in very good agreement with the previously reported B3LYP (TZVP basis set)⁴³ and plane wave PW91^{12,44} results. The energetically most favorable V₂O₄ structure is the cyclic isomer with a V–O₂–V ring and two vanadyl oxygen atoms in trans configuration. As has been pointed out in ref 45, the lowest-spin state is an open-shell singlet with one d-electron at each vanadium atom. It is 173 meV more stable than the triplet state, which is in good agreement with the previous PW91 calculations (177 meV)¹² and in qualitative agreement with the more reliable B3LYP results (112 meV).⁴⁵ The energy is obtained from the energy of the broken symmetry solution and the triplet state at the same geometry assuming $\langle \hat{S}^2 \rangle = 1$.

For the V₂O₅ and V₂O₄ clusters adsorbed on the κ -Al₂O₃(001) surface, a (2 × 1) unit cell is chosen and the vacuum is increased to 15 Å. A (2 × 2 × 1) k -point grid is used to sample the Brillouin zone. In ref 12, it was shown that on the α -Al₂O₃(0001) surface the cyclic V₂O₅ clusters are always less stable than the linear ones. The reason is that because of the V–O₂–V ring there are not very many coordination sites available for binding

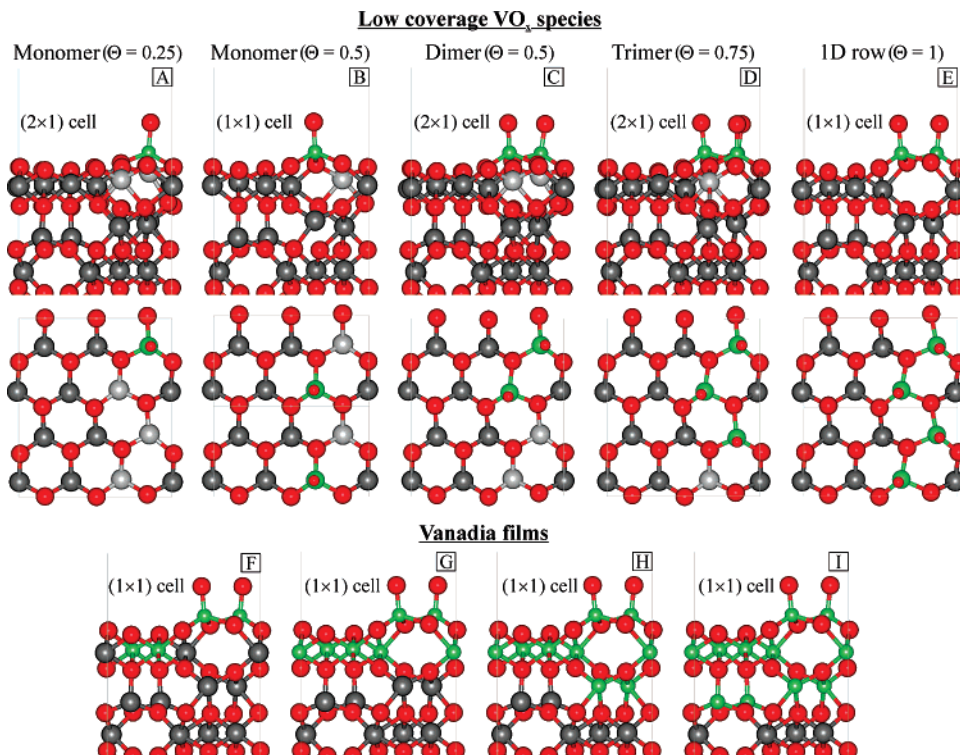


Figure 3. Vanadyl-terminated vanadia species supported on the κ -Al₂O₃(001) surface. (A–E) Side and top view of low-coverage vanadia aggregates ($\Theta \leq 1$ ML): monomers, dimers, trimers, and 1D vanadia rows. (F–I) Side view of high coverage ($\Theta > 1$ ML) vanadia films: (F) 2V-layer film, (G) 3V-layer film, (H) 4V-layer film, and (I) 5V-layer film, respectively. Vanadium atoms are green, oxygen atoms are red, and aluminum atoms are dark gray, whereas the topmost Al atoms are depicted light gray.

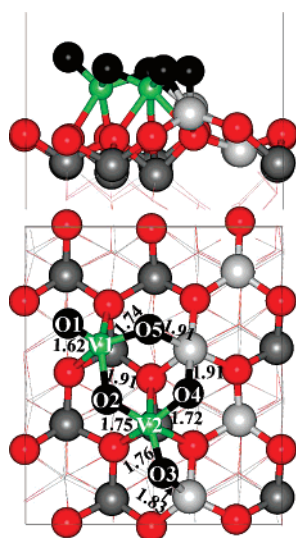


Figure 4. Side and top view of the most stable V₂O₅ cluster adsorbed on the κ -Al₂O₃(001) surface. Vanadium atoms are drawn green, aluminum atoms are dark gray, the topmost Al atoms are light gray, and oxygen atoms from the κ -Al₂O₃ surface are red, whereas those from a V₂O₅ unit are black. Bond lengths are in Å.

to the surface. Therefore, here only linear V₂O₅ clusters have been placed on the κ -surface and the most stable (dimeric) structure is shown in Figure 4.

All V₂O₄ clusters on the κ -Al₂O₃(001) surface are obtained by removing one oxygen atom from the most stable V₂O₅ cluster (Figure 4). Figure 5 shows their relaxed structures. There are five different oxygen atoms that can be removed: a vanadyl oxygen (O1), a bridging oxygen (O2) that is doubly coordinated to the vanadium sites V–O⁽²⁾–V, and three inequivalent interface Al–O⁽²⁾–V oxygen atoms (O3, O4, and O5). Replace-

ment of one of the two V atoms by an Al atom in a V₂O₄ cluster creates VO_{2.5}AlO_{1.5} species (i.e., monomers ($\Theta = 0.25$ ML) that are structurally different from those shown in Figure 3A). In both monomers, however, vanadium is in the V^V oxidation state. Hence, for the κ -Al₂O₃ support we use two different approaches to model monomeric and dimeric vanadia species.

D. Low-Coverage VO_x Species on α -Al₂O₃(0001) Surface. Results for vanadia films of various thicknesses (up to ~ 6 Å)¹¹ and for V₂O₅ and V₂O₄ clusters¹² supported on the α -Al₂O₃(0001) surface have been recently published. But monomeric and dimeric VO_x species constructed by replacement of Al atoms by V have not been investigated yet. In this work, we consider such models for the α -Al₂O₃(0001) surface, thus enabling the comparison with similar species on the κ -Al₂O₃ support (Section III B). Isolated VO_x sites that are created by replacing one of the outermost Al atoms in a (2 × 2) unit cell of the α -Al₂O₃(0001) slab ($A = 80$ Å²) by a O=V group are separated by 9.60 Å from the next-neighbor vanadyl groups. We refer to them as monomers type I (see Figure S1 in Supporting Information). This is very similar to the dispersion of the monomeric sites on κ -alumina at $\Theta = 0.25$ ML (see Figure 3A). Replacement of one additional Al atom in a nearest-neighbor position results in the formation of “dimeric” vanadia sites that are separated by a distance of 4.80 Å. We termed them pseudodimeric sites because they are not connected via a direct V–O–V bond. This contrasts with the dimeric sites on κ -Al₂O₃, which are separated by 3.1 Å and do share an oxygen atom (cf. Section III B). Similar to κ -Al₂O₃, monomers created by replacement of one of the two V atoms by an Al atom in the most stable V₂O₄ cluster adsorbed on the α -Al₂O₃(0001) surface,¹² are studied in this work. They are referred to as monomers type II. We also consider the reduction of all these systems by creating oxygen defects. All calculations employ a (3 × 3 × 1) *k*-point grid.

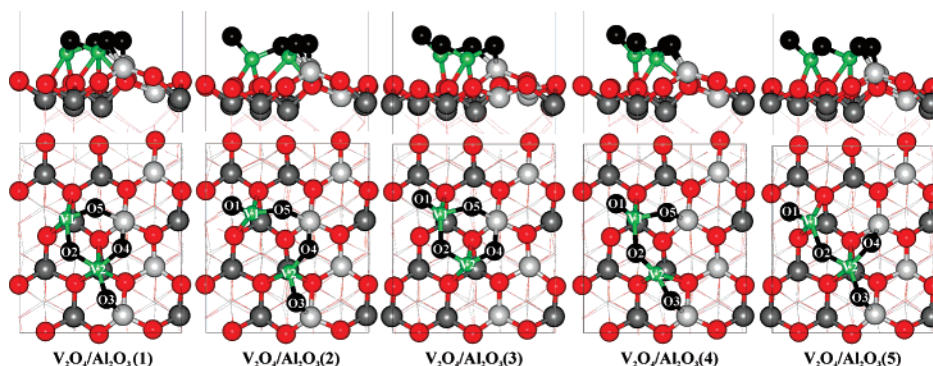


Figure 5. Optimized structures of the V_2O_4 clusters on the $\kappa\text{-Al}_2\text{O}_3(001)$ surface obtained upon removal of a single oxygen atom (number in parenthesis) from the most stable $V_2O_5/\kappa\text{-Al}_2\text{O}_3$ cluster.

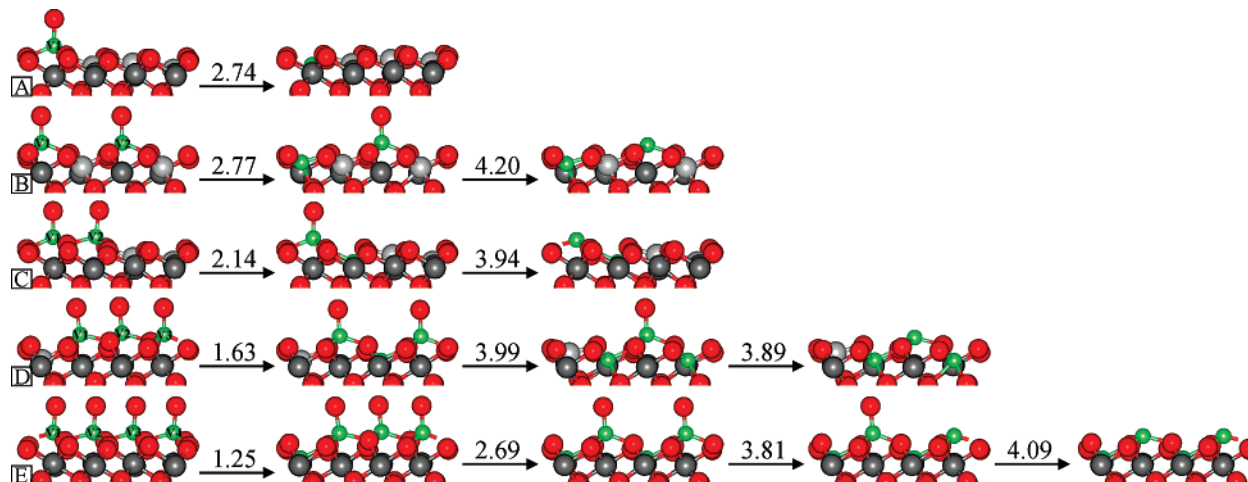


Figure 6. Reduction of low-coverage vanadia species: (A) monomers at $\Theta = 0.25$ ML, (B) monomers at $\Theta = 0.5$ ML, (C) dimers at $\Theta = 0.5$ ML, (D) trimers at $\Theta = 0.75$ ML, and 1D vanadia rows at $\Theta = 1$ ML. The vanadyl oxygen vacancy formation energy is given in eV. See Figure 3 for color coding.

IV. Results and Discussions

A. Reducibility of Vanadia Aggregates Created by Replacement. Isotopic-labeling studies of supported vanadia catalysts have shown that lattice oxygen atoms take part as reactive intermediates in oxidation reactions (Mars-van Krevelen mechanism).^{46,47} If we accept that the activity of the heterogeneous catalyst depends on its ability to release lattice oxygen, the E_f may be used as an indicator of its catalytic activity. Note that the trends in the enthalpy of this reduction reaction are not to be compared with the reducibility trends as deduced from temperature-programmed reduction experiments. In this technique, the catalyst is heated in a flow of hydrogen while monitoring the hydrogen consumption leading to the reduction of all reducible species (i.e., not only those at the surface). The results yield information on the kinetics of this reduction process.

We have previously shown that the crystalline $\alpha\text{-V}_2\text{O}_5(001)$ surface is much more reactive than the epitaxial vanadia films on an $\alpha\text{-Al}_2\text{O}_3(0001)$ support ($E_f \sim 2$ versus 4 eV/atom). This is due to the stabilization of the reduced surface V-sites by forming new V–O–V bonds with the V_2O_5 crystal layer underneath. Moreover, small dimeric species on $\alpha\text{-Al}_2\text{O}_3$ are more difficult to reduce ($E_f \sim 3$ eV/atom) than the $\alpha\text{-V}_2\text{O}_5(001)$ surface, but significantly easier than the supported vanadia films.^{48,11,12} The reason is the formation of a new V–O⁽³⁾–V bond at the vanadia/alumina interface of the dimeric species upon creation of the defect resulting in a four-membered V–O⁽³⁾–V ring.

In this work, we evaluate the energy to remove surface lattice oxygen atoms from vanadia aggregates supported on the

metastable $\kappa\text{-Al}_2\text{O}_3(001)$ surface and compare with the results obtained for the stable $\alpha\text{-Al}_2\text{O}_3(0001)$,^{10–12} thus gaining further insight into the role of the support structure.

1. Low-Coverage VO_x Species. We start our discussion by considering the initial reduction of low-coverage vanadia species by creating a single vanadyl oxygen defect. Figure 6 illustrates the structural relaxation induced by the subsequent removal of vanadyl oxygen atoms starting from fully vanadyl-covered monomeric and polymeric species supported on the $\kappa\text{-Al}_2\text{O}_3$ surface until their complete reduction. The corresponding vacancy formation energies before and after relaxation are summarized in Table 2.

Upon relaxation, the energy to remove a vanadyl oxygen atom from the isolated VO_x site at $\Theta = 0.25$ ML is lowered from 3.32 to 2.74 eV. The reduced V-center (V1) relaxes inward into the hole in the octahedral layer and forms one new V–O bond with an oxygen atom from the O⁵ layer beneath (see Figure 2 for layers labeling), thus recovering its tetrahedral coordination. The three topmost Al atoms (shown as light gray in Figure 6A) are also tetrahedrally coordinated. As a result, the $\kappa\text{-Al}_2\text{O}_3$ surface with the reduced monomeric VO_x sites becomes oxygen terminated. The defect formation energy of similarly dispersed monomers on $\alpha\text{-Al}_2\text{O}_3$ (monomer I, cf. Section 3.4) is 4.47 eV, that is, about 1.7 eV more costly (relaxation effects amount to ~ 0.1 eV), and the surface is metal-terminated. Increasing the coverage of monomeric species to $\Theta = 0.5$ ML on $\kappa\text{-Al}_2\text{O}_3$ does not influence the initial reduction of vanadyl oxygen atoms and the calculated $E_f = 2.77$ eV. In this case, half of the outermost Al atoms become tetrahedrally coordinated. Thus,

TABLE 2: Oxygen Vacancy Formation Energy E_f in eV Per $1/2O_2$ Molecule for the Initial and Subsequent Reduction of the Vanadia Aggregates on the κ - $Al_2O_3(001)$ Surface^a

structure	E_f^{Initial}	$E_f^{\text{Subsequent}}$
monomer ($\Theta = 0.25$ ML)	2.74 (3.32)	
monomer ($\Theta = 0.5$ ML)	2.77 (3.23)	4.20 (4.29)
dimer ($\Theta = 0.5$ ML)	2.14 (3.50)	3.94 (4.07)
trimer ($\Theta = 0.75$ ML)	1.63 (3.45)	3.99 (4.48)
		3.89 (4.02)
1D vanadia row ($\Theta = 1$ ML)	1.25 (3.48)	2.69 (3.85)
		3.81 (3.95)
		4.09 (4.37)
2V-layer film	3.31	4.00
3V-layer film	2.96	4.07
4V-layer film	2.49	3.93
5V-layer film	2.37	4.03
4V-layer reconstructed film	3.98	
5V-layer reconstructed film	3.98	

^a The values in parenthesis correspond to the formation energy of the unrelaxed structures.

decreasing the separation of the monomers on the κ -alumina surface from 9.77 to 4.88 Å (cf. Figure 3A,B) results in a very small change in the initial defect formation energy.

True dimeric species on κ - Al_2O_3 at $\Theta = 0.5$ ML (Figure 3C), which have a direct V–O–V bond, are by 0.56 eV less stable than the monomeric species at the same V-coverage (Figure 3B). In the latter, the two outermost Al atoms are 5-fold coordinated, whereas in the former they are 4- and 5-fold, respectively. Thus, low-coverage VO_x when supported on the κ - Al_2O_3 surface prefer to be as dispersed as possible. At higher VO_x coverages, however, formation of oligomeric species cannot be avoided. Upon removal of a single vanadyl oxygen atom, the dimeric species undergo a larger structure relaxation than the monomeric ones, which lowers the vacancy formation energy from 3.50 to 2.14 eV. The reduced V-center becomes octahedrally coordinated due to the formation of three V–O bonds with oxygen atoms of the oxygen layer O^5 beneath, while the two outermost Al atoms remain tetrahedrally and pyramidally coordinated, respectively. The initial defect formation energy of pseudodimeric sites on α - Al_2O_3 (cf. Section 3.4) is 4.34 eV with a relaxation contribution of ~ 0.1 eV only. The values of 2.74 and 2.14 eV compared to 4.47 and 4.34 eV for vanadia species at coverages up to 0.5 ML on the κ - and α - Al_2O_3 , respectively, demonstrate that the initial reduction of small aggregates on the metastable support is much more facile than on the stable one.

Upon the reduction of trimers, the energy decreases from 3.45 to either 1.63 or 2.02 eV depending on whether the central or a terminal vanadyl oxygen has been removed (V2 and V1 in Figure 6D, respectively). In all cases, the reduced V-atoms become octahedrally coordinated. However, relaxation effects change the coordination of the topmost aluminum atom to tetrahedrally when the reduced site is at the end of the trimer and remains pyramidally otherwise. Further decrease of the initial defect formation energy is found for the 1D vanadia rows (1.25 eV only). The unrelaxed value is 3.48 eV, and structure relaxation results in octahedrally coordinated reduced sites. As the length of the polymeric species increases from two to three and finally to 1D zigzag chains, the initial reduction becomes more and more facile.

We continue our discussion by considering the subsequent reduction of low-coverage vanadia species on the metastable support. The formation of additional vanadyl oxygen defects becomes more difficult (about 4 eV) partly because of the repulsive interactions between defects (see Table 2). The energy

is approximately the same regardless of the size (i.e., length) of the aggregates. Specifically, subsequent reduction of the monomeric species at $\Theta = 0.5$ ML, which leaves the surface metal terminated (Figure 6B), requires 4.20 eV (relaxation effects amount to less than 0.1 eV). The resulting fully reduced VO_x/κ - Al_2O_3 surface is buckled. Comparison of the initial and subsequent defect formation energies indicates that despite the large separation between two V centers of 4.88 Å, these monomers cannot be regarded as isolated species. In contrast, on the stable α - Al_2O_3 support the V-sites forming pseudodimers at $\Theta = 0.5$ ML can be considered to be isolated with an energy difference between the initial and subsequent reduction of 0.12 eV. The subsequent reduction of real dimeric species on κ - Al_2O_3 yields a metal-terminated surface that is buckled. The inward relaxation of two neighboring V-sites into the octahedral hole running along the [100] direction is not observed.

As far as the trimers are concerned, in the most stable structure the two reduced sites are not closest neighbors. The reduced centers (V1 and V3 in Figure 6D) do relax inward while increasing their coordination to 5-fold. Complete reduction of the trimer does not cause significant lattice relaxation and the surface is left metal-terminated (Figure 6D). This indicates that starting from the initially reduced polymeric species, further reduction would preferentially take place on next-nearest neighbors along the zigzag row resulting in the formation of a buckled layer of up and down metal sites. This is confirmed by the subsequent removal of vanadyl oxygen atoms from the 1D vanadia rows. That is, the creation of a second oxygen defect favors the alternation of defect sites. The reduced structure has two vanadium sites that moved inward in the octahedral hole (V1 and V3 in Figure 6E) and became 5-fold coordinated. These significant lattice rearrangements are accompanied by a decrease of the subsequent defect formation energy from 3.85 to 2.69 eV. Further reduction of the third (V2) and fourth (V4) vanadyl oxygen atoms is calculated to be as costly as for the neighboring sites of already reduced centers (~ 4 eV). Those V centers stay up maintaining the buckled layer of up and down metal sites. This is in contrast to γ - and α - $V_2O_5(001)$ for which starting from an isolated defect site the subsequent removal of neighboring vanadyl oxygen atoms along rows in the [010] direction is favored.^{48,49}

Two conclusions can be drawn. First, the removal of lattice oxygen atoms from the low-coverage vanadia species considered in this section is favored by the open structure of the metastable alumina support that facilitates relaxation and formation of new V–O bonds. Second, the (initial) reduction of polymeric VO_x species is more facile than that of monomers. The longer polymeric species are likely to be particularly easy to reduce. This might be correlated with the observed effect of vanadia surface density on the initial rate of alkene formation.^{5,50}

2. Vanadia Films. In this section, we consider the reducibility of vanadia films supported on the κ - $Al_2O_3(001)$ surface and compare with the results previously obtained for such films on the α - Al_2O_3 support.¹¹ For the 2V-layer film, a value of 3.31 eV is calculated for its initial reduction, which is significantly higher than the energy required for the initial reduction of low-coverage VO_x species. This reduction is less costly when thicker vanadium oxide films are formed. For instance, creation of a single defect requires 2.96 eV for the 3V-layer film and 2.49 and 2.37 eV for the 4V- and 5V-layer films, respectively. In all cases, the reduced V-center relaxes inward into the octahedral hole and increases its coordination to 5-fold by forming two new V–O bonds with oxygen atoms of the O^5 layer underneath.

In ref 11, we have shown that for the α -Al₂O₃ support formation of an oxygen defect is ~ 0.5 eV more costly for an ultrathin 1V-layer film (4.11 eV) than that for a thick 6V-layer film (3.59 eV). Thus, similar to the low-coverage vanadia aggregates, the oxygen defects are more easily formed in “epitaxially grown” vanadia films on the metastable κ -Al₂O₃(001) than on the stable α -Al₂O₃(0001) support. This is due to the presence of tetrahedral sites resulting in a much more open structure that facilitates lattice relaxation. Hereby, we establish a relation between the different support structures and the reducibility of alumina-supported vanadia aggregates.

Subsequent oxygen removal that results in a metal-terminated surface, however, requires ~ 4 eV regardless of the film thickness (see Table 2) and the support structure (κ - and α -Al₂O₃ phases differs by less than 0.1 eV).¹¹ For the removal of the vanadyl oxygen atom terminating the reconstructed 4V- and 5V-layer films (from which one vanadyl group is missing), a value of 3.98 eV is obtained. The similarity between this value and those corresponding to the subsequent reduction of the nonreconstructed films with the same thickness (cf. Table 2) is related to the equal composition of the topmost atomic layers, namely O=V–O₆–V₂–V₂–V–O₆– with one additional vanadium atom placed in the octahedral layer. It pops up from the V⁶ layer (reconstructed films) or, as in case of the unreconstructed films, it drops from the topmost V-layer (V¹).

Thus, the effect of the structure of the aluminum oxide support on the reducibility of supported vanadia species is suggested to be particularly significant at the initial reduction step (removal of first vanadyl oxygen) independent of the V-concentration.

B. Reducibility of Vanadia Clusters. *1. Adsorbed V₂O₅ Clusters on κ -Al₂O₃(001) Surface.* Figure 4 shows the most stable V₂O₅ cluster adsorbed on the κ -Al₂O₃(001) surface. It has one O=V bond, one V–O⁽²⁾–V bond, and three interface V–O⁽²⁾–Al bonds, where O⁽²⁾ indicates a 2-fold coordinated oxygen atom. These V–O⁽²⁾–Al interface-bridging bonds are only obtained when a V₂O₅ cluster is adsorbed on the surface, whereas all vanadia species created by replacement of Al atoms by V (see Section III B) on the κ -Al₂O₃ surface show only 3-fold coordinated oxygen atoms at the interface. Similar to the clusters on α -alumina, a V₂O₅ unit tends to bind as much as possible to the surface, thereby increasing the coordination of the undercoordinated surface Al and O atoms. One V atom (V1) is 5-fold coordinated and the other (V2) is 6-fold. Both of them occupy octahedral sites above Al atoms of the Al³ and Al⁴ layers. The oxygen atoms are approximately in one plane that follows the stacking sequence of oxygen layers. Moreover, its structure resembles that of the most stable V₂O₅ unit on α -alumina.¹² Closer inspection of the two models, however, shows that there are some differences. On α -Al₂O₃, the cluster has no vanadyl groups, the V–O–V bond contains a 3-fold coordinated oxygen atom, and two of the V–O⁽²⁾–Al bonds from the V₂O₅ unit are very short (1.67 and 1.68 Å), whereas in the V₂O₅ cluster on κ -Al₂O₃ the V–O⁽²⁾–Al bonds are in the 1.72–1.76 Å range. The adsorption energy of the V₂O₅/ κ -Al₂O₃ with respect to the most stable V₂O₅ gas-phase cluster is 6.47 eV. The coverage of V atoms per surface Al atoms is 0.5 ML, and the surface area is ~ 82 Å². For the two most stable clusters on the α -Al₂O₃(0001) support, adsorption energies of 6.80 and 6.67 eV were obtained.¹² The vanadium dispersion is also 0.5 ML and the surface area of 80 Å² is very similar.

The two less stable V₂O₅ clusters on the κ -Al₂O₃(001) surface found in the present study are shown in Figure S2 in Supporting Information. Their adsorption energies are 6.09 (cluster A) and 5.96 eV (cluster B).

TABLE 3: Oxygen Vacancy Formation Energy E_f in eV Per 1/2O₂ Molecule for the Most Stable V₂O₅/ κ -Al₂O₃ Cluster Structure, as Well as the Adsorption Energy E_{ad} (eV) for the V₂O₄ Clusters on the κ -Al₂O₃(001) Surface

O vacancy type	E_f	E_{ad}
V=O (O1)	2.27 (2.69)	6.71
V–O ⁽²⁾ –V (O2)	2.56 (3.73)	6.42
V–O ⁽²⁾ –Al (O3)	2.73 (4.31)	6.25
V–O ⁽²⁾ –Al (O4)	1.42 (3.20)	7.55
V–O ⁽²⁾ –Al (O5)	1.45 (3.23)	7.53

^a The values in parenthesis correspond to the formation energy of the unrelaxed structures.

2. V₂O₄ Clusters. We continue by considering oxygen removal from the V₂O₅ cluster (Figure 4) that results in five different V₂O₄/ κ -Al₂O₃ structures that are shown in Figure 5. Table 3 compiles the corresponding defect formation energies before and after relaxation. Table 3 also contains the adsorption energy of the V₂O₄ clusters on κ -Al₂O₃ given with respect to the gas-phase V₂O₄ cyclic-trans isomer.

Removal of the vanadyl oxygen O1 bound to the V1 site costs 2.69 eV, which upon relaxation is lowered to 2.27 eV. The resulting structure, V₂O₄/Al₂O₃(1), is very similar to the unrelaxed one (i.e., it preserves the V1–O2–V2–O4–Al–O5 ring), and all oxygen species from the V₂O₄ unit are in a plane parallel to the surface. No new bonds are formed; the V1–O2, V1–O5, and O5–Al bonds are shortened by 0.07, 0.05, and 0.10 Å, respectively, while the V2–O2 bond is stretched by 0.06 Å. The other bond lengths change by less than 0.02 Å. As a result of the bonding to the κ -Al₂O₃ surface, the V₂O₄ unit is stabilized by 6.71 eV.

The structure obtained upon removal of the O3 atom, V₂O₄/Al₂O₃(3), is quite similar to the former one. However, it undergoes significant lattice rearrangements accompanied by a decrease of the defect formation energy from 4.31 to 2.73 eV. In particular, the V1 atom loses one bond with a surface oxygen atom, while the coordination of the V2 site is reduced from 6-fold to 4-fold. This is caused by the large inward relaxation of the outermost Al directly bound to the O3 atom and consequent inward movement of the lattice oxygen connected to it. Thus, both vanadium sites become tetrahedrally coordinated and are no longer in the same plane. Similar to the V₂O₄/Al₂O₃(1) cluster, this V₂O₄ unit is very strongly adsorbed on the κ -surface (6.25 eV).

Removing the O2 atom from the V–O⁽²⁾–V bridge breaks the V1–O2–V2–O4–Al–O5 ring and yields a linear surface cluster V₂O₄/Al₂O₃(2) (see Figure 5). The same effect is obtained upon removal of O4 or O5 atoms from the interface V–O⁽²⁾–Al bonds. The large relaxation of the V₂O₄/Al₂O₃(2) structure lowers the vacancy formation energy from 3.73 to 2.56 eV. Here, the V2 atom moves upward and the bond with the lattice oxygen centered in the middle of the V1–O2–V2–O4–Al–O5 ring breaks up. As a result, the coordination of both V1 and V2 sites is reduced to 4-fold. This V₂O₄ cluster is also strongly bound to the alumina surface with a similar value for the adsorption energy (6.42 eV) as the other reduced clusters (see Table 3).

Interestingly, a very small amount of energy is required to remove one of the interface O4 and O5 atoms (i.e., 1.42 and 1.45 eV, respectively). Those oxygen atoms are bound to the outermost Al atom (4-fold coordinated in the bulk) that upon adsorption of the vanadia cluster became 5-fold coordinated. Significant structure relaxation upon oxygen removal is accompanied by ~ 1.8 eV decrease in the vacancy formation energy. All bond lengths change by less than 0.02 Å, except

for the bonds that involve the overcoordinated Al atom. In case of O4 removal, the O5–Al bond is shortened by 0.09 Å to a value of 1.82 Å, a typical Al^T–O distance in bulk κ -Al₂O₃. The same happens when the O5 atom is removed (i.e., O4–Al bond is shortened to 1.79 Å, while the V2–O2 is stretched by 0.07 Å). As a result, in both cases the Al ion nearly recovers its perfect tetrahedral bulk coordination. Hence, the larger values (7.55 and 7.53 eV) calculated for the adsorption energies of those two V₂O₄ clusters appear in line with the additional structure stabilization.

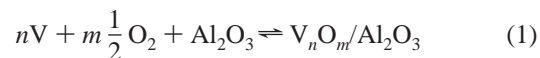
Removal of the vanadyl oxygen atom from the most stable monomeric site obtained by replacing one V by an Al atom in the V₂O₄/Al₂O₃(4) cluster requires 1.72 eV. In comparison with the initial reduction of the corresponding dimer (1.42 eV, cf. Table 3), reduction of such a monomeric V-site is by 0.3 eV more costly. This trend is confirmed for similarly modeled vanadia species on the α -Al₂O₃ support. The most stable monomer (monomer II, cf. Figure S1 in Supporting Information) is characterized by the presence of two differently coordinated interface oxygen atoms and no O=V groups. Removal of a bridging oxygen atom at the V–O⁽²⁾–Al interface costs 4.16 eV, whereas 5.53 eV are required for reduction of a bridging oxygen at the V–O⁽³⁾–Al interface. The formation energy of a defect at the V–O⁽²⁾–Al interface of the corresponding dimer is 2.79 eV (ref 12), which again indicates a more facile reduction of alumina-supported dimeric species as compared to monomeric ones.

In regard to the energy for creating oxygen defects at the surface of low-coverage alumina-supported vanadia aggregates, the following conclusions can be drawn. Reduction of monomers and dimers modeled by clusters adsorbed on the κ -Al₂O₃(001) surface requires between 1.42 and 2.73 eV per 1/2O₂ molecule. These species ($\Theta \leq 0.5$ ML) are anchored at the surface with V–O⁽²⁾–Al interface bonds. For low-coverage species ($\Theta \leq 1$ ML) but a different nature of the interface (V–O⁽³⁾–Al), the energy varies between 1.25 and 2.77 eV with the reduction of the monomer being the most difficult (see Table 2). On the stable α -Al₂O₃(0001) surface, the energy cost for the formation of a single oxygen defect at the V–O⁽²⁾–Al interface lies in the range of 2.79 – 4.77 eV,¹² whereas at the V–O⁽³⁾–Al interface the energy varies between 4.34 and 5.53 eV. Thus, oxygen defects can be more easily created on small vanadia aggregates supported on the metastable κ -Al₂O₃ than on the stable α -Al₂O₃ surface.

Formation of a (neutral) oxygen defect in all vanadia aggregates supported on the κ -Al₂O₃(001) surface leaves two electrons in the system, which occupy d-states localized on one V-site that becomes V^{III}(d²), while the second V-site remains in a V^V(d⁰) configuration. This is different from the reduction of dimeric species on the α -Al₂O₃ support for which formation of a four-membered V–O₂–V ring upon lattice relaxation results in a pair of V^{IV}(d¹) sites. The vacancy formation energy was 2.79 eV,¹² whereas for such species on the κ -Al₂O₃ support we obtained a much lower value (1.42 eV). This shows that low-defect formation energies can be obtained when substantial relaxation effects occur that not necessarily yield to the formation of a V^{IV}(d¹) pair.

C. Thermodynamic Stability of Vanadia Aggregates on κ -Al₂O₃(001) Surface. As with our recent studies on vanadium oxides supported on the α -Al₂O₃(0001) surface,^{11,12} we apply statistical thermodynamics to take into account the effect of oxygen partial pressure and vanadium concentration at a given temperature on the stability of the supported vanadia aggregates on the metastable κ -Al₂O₃(001) surface.

Using the same notation as in ref 11, we consider the equilibrium



with the accompanying change in the surface-related free energy $\Delta\gamma$

$$\Delta\gamma(T, p) = \frac{1}{A} [\Delta E - n\Delta\mu_V - m\Delta\mu_O] \quad (2)$$

The reaction energy ΔE is the energy required to form the alumina-supported vanadium oxide from the κ -Al₂O₃ support, metallic vanadium and oxygen. In calculating $\Delta\gamma$, we use DFT total energies of the vanadia-supported slab, the clean κ -Al₂O₃(001) surface, the oxygen molecule, and the metallic body-centered cubic bulk vanadium, neglecting the vibrational contributions of the solid components. A is the surface area. The chemical potential differences $\Delta\mu_i$ are expressed as

$$\Delta\mu_V(T, a_V) = \mu_V(T, a_V) - E_V \quad (3)$$

$$\Delta\mu_O(T, p) = \frac{1}{2} [\mu_{O_2}(T, p) - E_{O_2}] \quad (4)$$

where μ_i is the chemical potential and a_V and p_{O_2} are the vanadium activity and the oxygen partial pressure, respectively. From a practical point of view, the vanadium activity can be varied by controlling the amount of the evaporated vanadium forming the oxide and is related to the concentration through the activity coefficient.⁵¹ V and O₂ particle reservoirs are in equilibrium with bulk V and O₂ in the gas phase. Two independent variables, $\Delta\mu_V$ and $\Delta\mu_O$, control the formation of vanadia aggregates.

The most favorable structure for a given set of vanadium and oxygen chemical potentials is the one that minimizes the surface free energy $\Delta\gamma$ according to eq 2. The resulting phase diagram is shown in Figure 7 with values of the oxygen potential related to the oxygen pressure at $T = 800$ K.

At the highest vanadium chemical potentials, the thickest film considered forms (i.e., 5V-layer film, cf. Figure 7a). The same result was found for the vanadia films on the α -Al₂O₃ surface¹¹ (see Figure 8). At very reducing conditions ($\Delta\mu_O \lesssim -2.4$ eV) and still high $\Delta\mu_V$ values, the film obtained upon removal of a single vanadyl O-atom from this fully vanadyl-covered thick film becomes stable (Figure 7b). Upon gradually decreasing the $\Delta\mu_V$ values, a reconstructed film with the same thickness (5V layers) is stable (Figure 7c). As was mentioned before, this vanadia film has the same composition of the outermost layers (O=V–O₆–V₂–V₂–V–O₆) as the reduced unreconstructed one (Figure 7b), as well as a very similar vacancy formation energy (3.98 eV). Further decreasing the vanadium potential leads to stabilization of the reconstructed thinner 4V-layer films (Figure 7d). Again, we note similarities with the calculated phase diagram for the vanadia films on α -Al₂O₃ support where in an intermediate range of $\Delta\mu_V$ values similarly reconstructed structures are predicted to form.¹¹ Further reducing the $\Delta\mu_V$ values results in formation of 1 ML thick structures. That is, similar to α -Al₂O₃, no aggregates with intermediate thicknesses are observed and the film becomes as thick as the vanadium supply allows.

However, the plots differ significantly at low-vanadium chemical potential that is not sufficient for the formation of vanadia bulk phases. Figure 7 shows all stable low-coverage ($\Theta \leq 1$ ML) vanadia species on the κ -Al₂O₃(001) surface. As

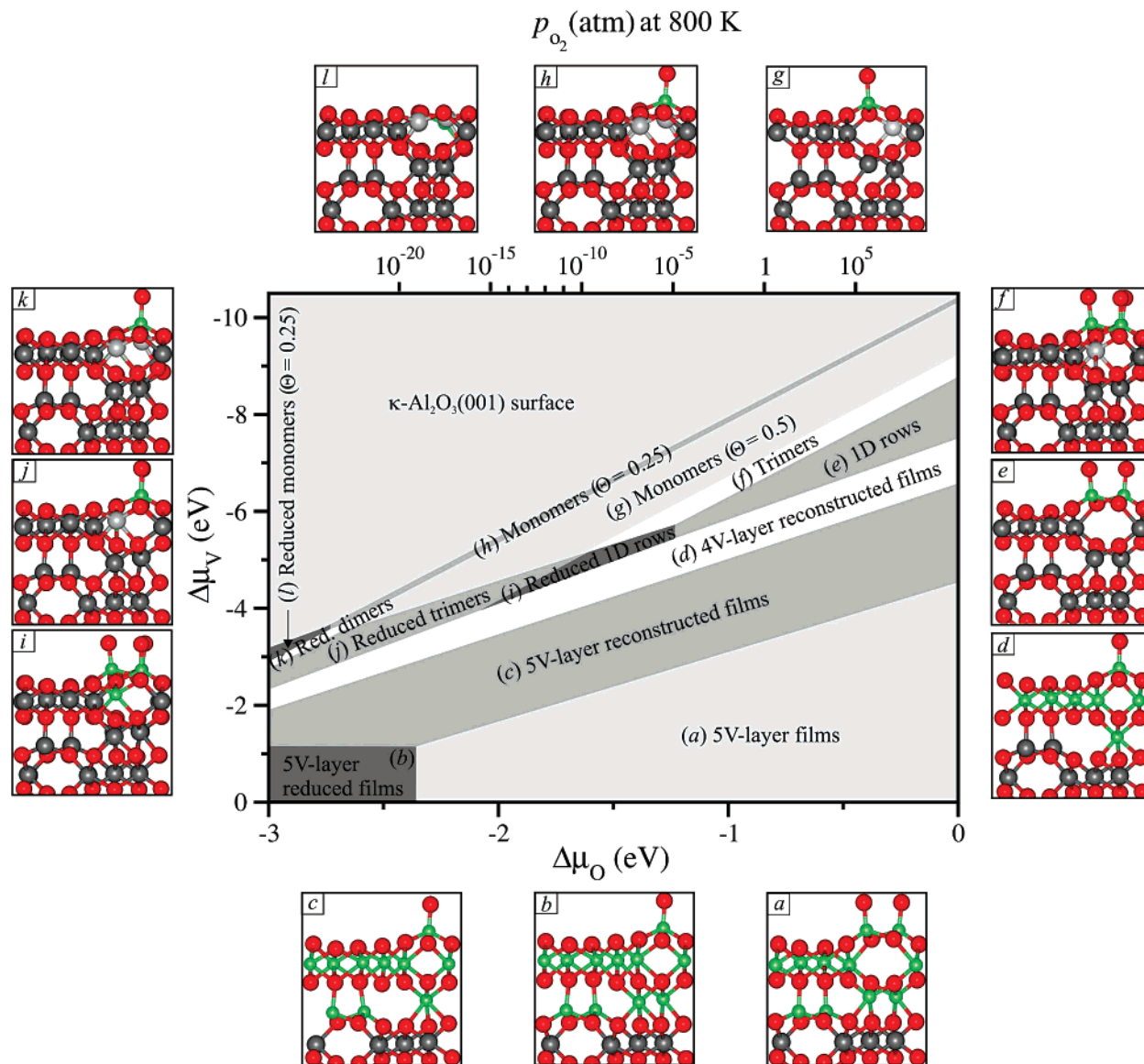


Figure 7. Phase diagram as a function of the $\Delta\mu_{\text{O}}$ and $\Delta\mu_{\text{V}}$ chemical potentials for vanadia aggregates supported on the $\kappa\text{-Al}_2\text{O}_3(001)$ surface. $\Delta\mu_{\text{O}}$ is translated into a pressure scale at $T = 800$ K. See Section IV C for explanation of panels a–l.

$\Delta\mu_{\text{V}}$ decreases, for high $\Delta\mu_{\text{O}}$ values ($\Delta\mu_{\text{O}} \gtrsim -1.25$ eV, which corresponds to $p \gtrsim 10^{-5}$ atm at 800 K), fully vanadyl-terminated 1D vanadia rows (Figure 7e), trimers (Figure 7f), and monomers at $\Theta = 0.5$ and 0.25 ML (Figure 7g and 7h, respectively) are predicted to be thermodynamically stable. We note that the monomeric species at $\Theta = 0.5$ ML (Figure 3B) compete with the dimeric ones at the same coverage (Figure 3C) but are 0.56 eV more stable. Thus, the vanadyl-covered dimer does not show up in the stability plot. Interestingly, there are regions at which the partially reduced 1D rows (Figure 7i) and trimers (Figure 7j) are energetically favorable under UHV conditions. At even lower oxygen pressure, the partially reduced dimers (Figure 7k) and monomers at $\Theta = 0.25$ ML (Figure 7l) are also stabilized.

All low-coverage vanadia species supported on the $\kappa\text{-Al}_2\text{O}_3(001)$ surface have $\text{V}-\text{O}^{(3)}-\text{Al}$ interface bonds. Despite the facile reduction of differently anchored ($\text{V}-\text{O}^{(2)}-\text{Al}$) dimeric species (cf. Figures 4 and 5), they (and their reduced counterparts) are not predicted to be thermodynamically stable. This is a major difference compared to vanadia on the $\alpha\text{-Al}_2\text{O}_3$ surface for which adsorbed V_2O_5 and V_2O_4 clusters (with $\text{V}-\text{O}^{(2)}-\text{Al}$ interface bonds) are calculated to be stable.¹² The structure of the α -support does not allow for the formation of differently anchored dimeric species.

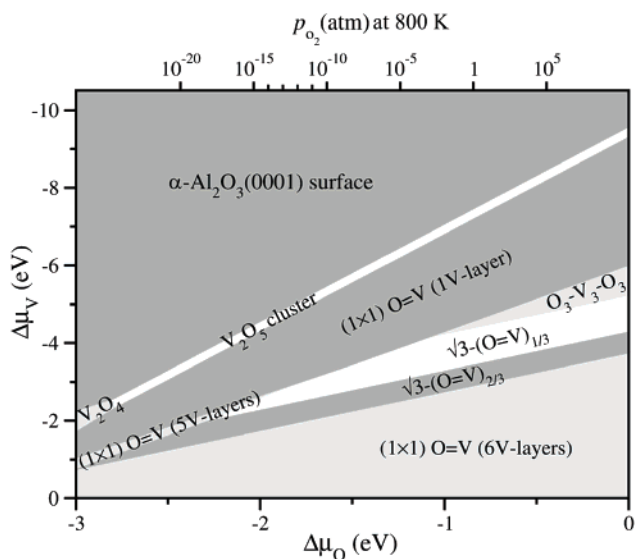


Figure 8. Phase diagram as a function of the $\Delta\mu_{\text{O}}$ and $\Delta\mu_{\text{V}}$ chemical potentials for vanadia aggregates supported on the $\alpha\text{-Al}_2\text{O}_3(0001)$ surface. $\Delta\mu_{\text{O}}$ is translated into a pressure scale at $T = 800$ K.

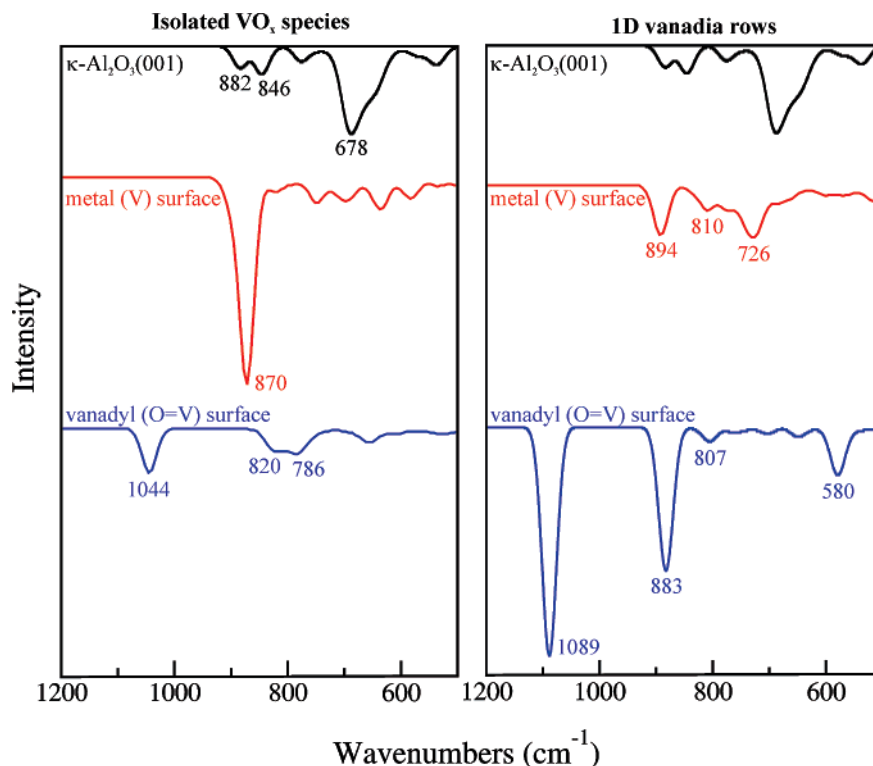


Figure 9. Calculated frequencies for the IR active vibrations of the monomeric species at $\Theta = 0.5$ ML (left panel) and 1D vanadia rows at $\Theta = 1$ ML (right panel) supported on the κ - $\text{Al}_2\text{O}_3(001)$ surface. The spectrum of clean surface is drawn in black, the fully reduced metal (V) and the vanadyl- (O=V) terminated surfaces are in red and blue, respectively.

The phase diagram of the vanadia aggregates on the stable α - $\text{Al}_2\text{O}_3(0001)$ surface is shown in Figure 8. In addition to the V_nO_m films and clusters that appear on the stability plots published in our recent studies,^{11,12} we have yet included the clean alumina surface as well as the low-coverage VO_x species presented in Section III D. However, our calculations indicate that none of the two different monomeric species at $\Theta = 0.25$ ML would form, and the only stable low-coverage vanadia are dimers. This is another major difference compared to the κ -alumina support for which monomers at two different VO_x loadings are stable. Hence, the present study demonstrates that the support structure does affect the structure of the catalyst.

An important difference between the low-coverage VO_x species on α - Al_2O_3 and those on κ - Al_2O_3 is the stability of the reduced systems. The α -alumina-supported reduced dimers would only become stable for $\Delta\mu_{\text{O}} \lesssim -2.8$ eV, which corresponds to a pressure of 10^{-12} atm at very high temperatures (1200 K). This correlates with the more facile reduction of κ - Al_2O_3 -supported vanadia compared to α - Al_2O_3 .

Characteristic features of the experimental model catalysts prepared by vanadium evaporation under UHV conditions⁸ are the presence of V in an average oxidation state of V^{III} (as in V_2O_3) and the existence of surface vanadyl groups. The oxidation state of V^{V} of the surface V-atoms is only detectable on a flat V_2O_3 surface if spectra are taken at grazing angles.^{52,53} For vanadia aggregates on κ - Al_2O_3 , we predict low-coverage polymeric species to be partially reduced in UHV and $T \gtrsim 800$ K (i.e., to have V^{V} and V^{III} centers). As the V-coverage increases and three-dimensional (3D) structures (films) form, V^{III} centers become prevalent in the bulk but will not be accessible for reactant molecules.

D. Vibrational Analysis. We have calculated the vibrational spectra of selected structures (e.g., monomers at $\Theta = 0.5$ ML and 1D vanadia rows having exclusively $\text{V}-\text{O}^{(3)}-\text{Al}$ interface bonds) as well as the V_2O_5 and the V_2O_4 clusters anchored at

the κ - $\text{Al}_2\text{O}_3(001)$ surface with $\text{V}-\text{O}^{(2)}-\text{Al}$ bonds. Figure 9 shows the frequencies of the IR active vibrations of the clean κ - $\text{Al}_2\text{O}_3(001)$ surface and both the fully reduced and the vanadyl- (O=V) terminated monomers and 1D rows. For the clean κ -surface, we have assigned the most intense broad band at 678 cm^{-1} to the Al_2O_3 bulk modes and the two weak bands at 882 and 846 cm^{-1} to $\text{Al}^{\text{T}}-\text{O}$ stretching modes. The vibration at 882 cm^{-1} involves exclusively the tetrahedrally coordinated Al atoms. It is shifted by $\sim 45\text{ cm}^{-1}$ toward higher wavenumbers as compared to the highest IR active mode of the clean α - Al_2O_3 surface (837 cm^{-1}). This is because the $\text{Al}^{\text{T}}-\text{O}$ bond distances (1.75 – 1.79 \AA), which occur only in κ - Al_2O_3 , are much shorter than the $\text{Al}^{\text{O}}-\text{O}$ distances (1.84 – 1.99 \AA) that are common for both Al_2O_3 phases.

Upon creation of monomeric V sites, a very sharp and intense band at 870 cm^{-1} emerges, which is assigned to $\text{V}-\text{O}^{(3)}-\text{Al}$ coupled with $\text{Al}-\text{O}$ stretching modes of the whole slab. Additionally, the intensity of the broad Al_2O_3 bulk peak significantly decreases. When the surface is oxidized and covered with vanadyl oxygen atoms, the calculated vibrational spectrum shows a new band at 1044 cm^{-1} , which is the typical vanadyl bond stretch. It is lower than that calculated for the $\text{V}_2\text{O}_5(001)$ single crystal surface (1079 – 1095 cm^{-1})¹⁰ and the thin films on the α - $\text{Al}_2\text{O}_3(0001)$ surface (1058 , 1076 cm^{-1}).¹⁰ A very broad peak with two maxima at 820 and 786 cm^{-1} is assigned to $\text{V}-\text{O}^{(3)}-\text{Al}$ vibration strongly coupled with $\text{Al}-\text{O}$ stretching modes (red-shifted as compared to the metal-terminated model) and to pure $\text{Al}-\text{O}$ stretching modes, respectively.

Calculated IR spectra of the 1D vanadia rows do not show IR active $\text{V}-\text{O}^{(3)}-\text{V}$ modes. For the metal-terminated surface, the highest frequency at 894 cm^{-1} is a pure $\text{Al}-\text{O}$ stretching, mainly involving tetrahedral Al^{T} sites, whereas the one at 810 cm^{-1} includes all Al atoms in the slab. Similar to the isolated sites, a very intense band at 1089 cm^{-1} appears in the spectrum

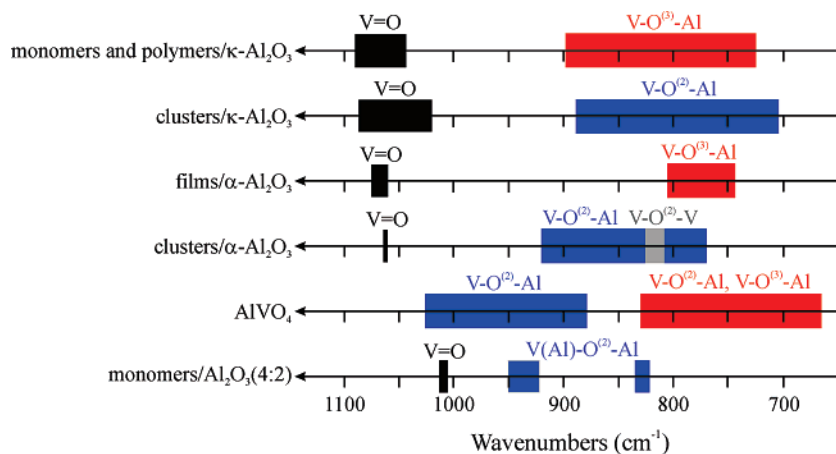


Figure 10. Harmonic vibrational frequencies of monomeric and polymeric vanadia species and clusters on the metastable κ - $\text{Al}_2\text{O}_3(001)$ surface (this work), vanadia films and clusters on the stable α - $\text{Al}_2\text{O}_3(0001)$ surface,¹² bulk AlVO_4 ,⁵⁴ and a cluster model for $\text{O}=\text{V}(\text{OAl})_3$ sites on alumina with 4-fold coordinated Al and 2-fold coordinated O atoms (4:2 coordination).⁵⁵

of the vanadyl-terminated vanadia rows. It is due to the in-phase stretching of the two vanadyl groups and is shifted toward higher wavenumbers as compared to the $\text{O}=\text{V}$ mode of monomers ($\Theta = 0.5$ ML). Slightly less intense is the band at 883 cm^{-1} , which is assigned to $\text{V}-\text{O}^{(3)}-\text{Al}$ vibrations coupled with stretching of $\text{Al}-\text{O}$ bonds that extend up to the Al^7 layer (cf. Figure 2). The largest displacements within the alumina framework correspond to stretching of the tetrahedrally coordinated aluminum atoms.

Furthermore, neither the dimer nor its reduced counterpart anchored at the surface via $\text{V}-\text{O}^{(2)}-\text{Al}$ interface bonds show bands above 900 cm^{-1} . Similar to the 883 cm^{-1} band for the 1D vanadia rows (with $\text{V}-\text{O}^{(3)}-\text{Al}$ bonds), these systems show bands at 858 cm^{-1} (V_2O_5) and 856 and 888 cm^{-1} (V_2O_4) assigned to interface vibrations coupled with $\text{Al}-\text{O}$ stretching. However, the nature of the interface bonds is different. Additionally, vanadyl bond stretch at 1020 (V_2O_5) and 1087 cm^{-1} (V_2O_4), as well as $\text{V}-\text{O}^{(2)}-\text{Al}$ vibrations strongly coupled with $\text{Al}-\text{O}$ stretching of the whole slab appear at $\sim 715\text{ cm}^{-1}$.

Frequency calculations of thin vanadia films supported on α - $\text{Al}_2\text{O}_3(0001)$ surface¹⁰ did not give rise to bands above 805 cm^{-1} (see Figure 10). In bulk AlVO_4 , in which oxygen atoms are 2-fold coordinated and form $\text{V}-\text{O}^{(2)}-\text{Al}$ bonds vibrations in the 1025 – 882 cm^{-1} region (Figure 10) were obtained and indeed assigned to $\text{V}-\text{O}^{(2)}$ stretch.⁵⁴ The shortest $\text{V}-\text{O}^{(2)}-\text{Al}$ bonds are 1.67 \AA and belong to rings composed of alternating oxygen and metal atoms. Moreover, a surface-localized $\text{V}-\text{O}^{(2)}-\text{Al}$ vibration at 922 cm^{-1} was obtained for the most stable V_2O_5 cluster adsorbed on the α - $\text{Al}_2\text{O}_3(0001)$ surface, which arises from the presence of short $\text{V}-\text{O}^{(2)}$ bonds (1.67 and 1.68 \AA) at the interface.¹² The bands at 858 cm^{-1} for the V_2O_5 cluster on κ - Al_2O_3 reveal that the structure of the support and in particular the presence of tetrahedral sites affects the interface vibrations. These dimeric species have a similar structure to the corresponding ones on α - Al_2O_3 ; however, they do not have any short $\text{V}-\text{O}^{(2)}$ bonds (see Figure 4). Their vibration in contrast to $\text{V}_2\text{O}_5/\alpha$ - Al_2O_3 is not surface-localized.

One puzzling question concerning alumina-supported vanadia catalysts is the nature of the 945 cm^{-1} band observed in the IR spectra of model systems as well as in the Raman spectra of powder samples.^{6,8,55} It was claimed that this mode is due to $\text{V}-\text{O}-\text{V}$ vibrations and therefore used as a fingerprint for the so-called “polymeric vanadia species”.⁶ In ref 8, it was suggested that this vibration is localized at the interface and

involves V, O, and Al ions. A vibrational study of alumina-supported vanadium oxides modeled by a cluster containing an $\text{O}=\text{V}(\text{OAl})_3$ unit with 2-fold coordinated oxygen atoms at the $\text{V}-\text{O}-\text{Al}$ interface and tetrahedrally coordinated aluminum atoms, revealed strong vibrational coupling between the in-phase $\text{V}-\text{O}^{(2)}-\text{Al}$ mode and the $\text{Al}-\text{O}-\text{Al}$ framework.⁵⁵ The authors reported four intense vibrations involving the $\text{V}-\text{O}-\text{Al}$ interface in the 955 – 925 cm^{-1} region with $\text{V}-\text{O}^{(2)}$ bonds of 1.77 and 1.78 \AA (cf. Figure 10).

Thus, based on the vibrational spectra summarized in Figure 10, we conclude that the presence of $\text{V}-\text{O}^{(2)}-\text{Al}$ interface bonds as a structural element of alumina-supported vanadia catalysts can not guarantee the appearance of a band at $\sim 950\text{ cm}^{-1}$ and that additional factors, such as the $\text{V}-\text{O}^{(2)}$ bond lengths, couplings, and the specific oxide support structure play a role. For κ -alumina-supported vanadia species, both $\text{V}-\text{O}^{(2)}-\text{Al}$ and $\text{V}-\text{O}^{(3)}-\text{Al}$ interface bonds give rise to bands in the same range (below $\sim 900\text{ cm}^{-1}$). This discussion also indicates that on the basis of the structure of models that produced the $\sim 950\text{ cm}^{-1}$ band, the nature of the interface cannot be unequivocally assigned.

V. Summary and Conclusions

Low-coverage vanadia species (monomers, dimers, trimers, and 1D vanadia rows) as well as vanadium oxide films of varying thickness supported on the κ - $\text{Al}_2\text{O}_3(001)$ surface have been investigated by DFT combined with statistical thermodynamics. The results are compared to those obtained for α - Al_2O_3 -supported species.

The vanadia/ κ -alumina phase diagram as a function of oxygen partial pressure and vanadium activity shows that at high values of the vanadium chemical potential, vanadia films would become as thick as the vanadium supply allows. The presence of vanadyl groups is a prevalent feature of the film termination rendering the oxidation state of vanadium V^{V} for the surface atoms and V^{III} for the atoms in the bulk of these 3D structures. This is similar to what has been predicted for the α - $\text{Al}_2\text{O}_3(0001)$ support.¹¹ A major difference appears at low $\Delta\mu_{\text{V}}$ values. On κ -alumina, low-coverage monomeric and polymeric species are anchored exclusively via $\text{V}-\text{O}^{(3)}-\text{Al}$ interface bonds, whereas on α -alumina only species with $\text{V}-\text{O}^{(2)}-\text{Al}$ bonds are stabilized. Moreover, under typical reducing conditions (UHV and high temperatures (e.g., $T \gtrsim 800\text{ K}$)), low-coverage aggregates on

κ -Al₂O₃ are partially reduced (i.e., they expose V^V and V^{III} centers). This correlates with defect formation energy values for the initial removal of lattice oxygen in the range of 1.25–2.74 eV. The reduction energy decreases as oligomers of increasing length form and reaches a minimum (1.25 eV) for the 1D rows. In contrast, on the α -Al₂O₃(0001) surface, the only stable low-coverage VO_x species are dimers with V–O⁽²⁾–Al interface bonds and a defect formation energy of 2.8 eV.

The supported vanadia catalysts are characterized by the ability to release lattice oxygen in Mars-van Krevelen-type oxidation reactions. If we accept that the catalytic activity depends on the catalyst's reducibility, the energy of oxygen defect formation may be used as an indicator of its catalytic performance. Hence, systems with low thermodynamic stability of lattice oxygen (i.e., small defect formation energy) are likely to perform better. Our findings indicate that the vanadyl-terminated low-coverage species on κ -Al₂O₃, which possess significantly labile oxygen atoms, are expected to exist at catalytically relevant conditions, namely atmospheric pressure and a temperature range of 500–800 K ($\Delta\mu_{\text{O}} = -0.50$ to -0.85 eV). Thus, the present study suggests that the VO_x/ κ -Al₂O₃ species are likely to show higher reactivity than the stable species on the α -Al₂O₃ support.

We have found that at a given VO_x loading, the reactivity of the supported vanadia species is influenced by the alumina support structure. Compared to α -Al₂O₃, the presence of tetrahedrally coordinated Al sites (25%) in κ -Al₂O₃ results in a much more open structure that facilitates significant defect-induced lattice relaxations. We expect that similar results will be obtained for vanadia supported on other metastable alumina phases such as γ -Al₂O₃ and on the unique structure of the ultrathin aluminum oxide film on NiAl(110).

Using the calculated vibrational spectra of dimeric species anchored via V–O⁽²⁾–Al interface bonds at the α - and κ -Al₂O₃ supports, we show that the sole presence of such bonds at the vanadia/alumina interface does not necessarily lead to surface-localized vibrations at ~ 950 cm⁻¹, and that the existence of tetrahedral sites affects the spectra.

Acknowledgment. This work has been supported by Deutsche Forschungsgemeinschaft (Sonderforschungsbereich 546). T.K.T. acknowledges the support from the Fonds der Chemischen Industrie and the International Max Planck Research School "Complex Surfaces in Materials Science". We thank V. Brázdová for providing the structure of one of the monomeric species supported on α -Al₂O₃ (monomer II), and R. Fortrie for insightful comments. V.G.P. thanks C. Ruberto and B. I. Lundqvist for useful discussions. The calculations were carried out on the IBM p690 system of the Norddeutscher Verbund für Hoch- und Höchstleistungsrechnen (HLRN).

Supporting Information Available: Monomeric VO_x species supported on the α -Al₂O₃(0001) surface, optimized structures of the second and third most stable V₂O₅ clusters on the κ -Al₂O₃(001) surface, table of total energies for all structures studied, and coordinates of the thermodynamically stable structures in Figure 7. This material is available free of charge via the Internet at <http://pubs.acs.org>.

References and Notes

- Mamedov, E. A.; Corberan, V. C. *Appl. Catal., A* **1995**, *127*, 1.
- Blasco, T.; Nieto, J. M. L. *Appl. Catal., A* **1997**, *157*, 117.
- Bañares, M. A. *Catal. Today* **1999**, *51*, 319.
- Bañares, M. A.; Huerta, M. V. M.; Gao, X.; Fierro, J. L. G.; Wachs, I. E. *Catal. Today* **2000**, *61*, 295.
- Khodakov, A.; Olthof, B.; Bell, A. T.; Iglesia, E. *J. Catal.* **1999**, *181*, 205.
- Weckhuysen, B. M.; Keller, D. E. *Catal. Today* **2003**, *78*, 25.
- Wachs, I. *Catal. Today* **2005**, *100*, 79.
- Magg, N.; Giorgi, J. B.; Schroeder, T.; Bäumer, M.; Freund, H.-J. *J. Phys. Chem. B* **2002**, *106*, 8756.
- Magg, N.; Giorgi, J. B.; Hammoudeh, A.; Schroeder, T.; Bäumer, M.; Freund, H.-J. *J. Phys. Chem. B* **2003**, *107*, 9003.
- Brázdová, V.; Ganduglia-Pirovano, M. V.; Sauer, J. *Phys. Rev. B* **2004**, *69*, 165420.
- Todorova, T. K.; Ganduglia-Pirovano, M. V.; Sauer, J. *J. Phys. Chem. B* **2005**, *109*, 23523.
- Brázdová, V.; Ganduglia-Pirovano, M. V.; Sauer, J. *J. Phys. Chem. B* **2005**, *109*, 23532.
- Jaeger, R. M.; Kuhlbeck, H.; Freund, H.-J.; Wuttig, M.; Hoffmann, W.; Franchy, R.; Ibach, H. *Surf. Sci.* **1991**, *259*, 235.
- Libuda, J.; Winkelmann, F.; Bäumer, M.; Freund, H.-J.; Bertrams, T.; Neddermeyer, H.; Müller, K. *Surf. Sci.* **1994**, *318*, 61.
- Frank, M.; Wolter, K.; Magg, N.; Heemeier, M.; Kühnemuth, R.; Bäumer, M.; Freund, H.-J. *Surf. Sci.* **2001**, *492*, 270.
- Ceballos, G.; Song, Z.; Pascual, J. I.; Rust, H.-P.; Conrad, H.; Bäumer, M.; Freund, H.-J. *Chem. Phys. Lett.* **2002**, *359*, 41.
- Klimenkov, M.; Nepijko, S.; Kuhlbeck, H.; Freund, H.-J. *Surf. Sci.* **1997**, *385*, 66.
- Kulawik, M.; Nilius, N.; Rust, H.-P.; Freund, H.-J. *Phys. Rev. Lett.* **2003**, *91*, 256101.
- Stierle, A.; Renner, F.; Streitl, R.; Dosch, H.; Drube, W.; Cowie, B. C. *Science* **2004**, *303*, 1652.
- Kresse, G.; Schmid, M.; Napetschnig, E.; Shishkin, M.; Köhler, L.; Varga, P. *Science* **2005**, *308*, 1440.
- Schmid, M.; Shishkin, M.; Kresse, G.; Napetschnig, E.; Varga, P.; Kulawik, M.; Nilius, N.; Rust, H.-P.; Freund, H.-J. *Phys. Rev. Lett.* **2006**, *97*, 046101.
- Wolverton, C.; Hass, K. C. *Phys. Rev. B* **2000**, *63*, 024102.
- Paglia, G.; Buckley, C. E.; Rohl, A. L.; Hunter, B. A.; Hart, R. D.; Hanna, J. V.; Byrne, L. T. *Phys. Rev. B* **2003**, *68*, 144110.
- Paglia, G.; Rohl, A. L.; Buckley, C. E.; Gale, J. D. *Phys. Rev. B* **2005**, *71*, 224115.
- Pinto, H. P.; Nieminen, R. M.; Elliott, S. D. *Phys. Rev. B* **2004**, *70*, 125402.
- Krokidis, X.; Raybaud, P.; Gobichon, A.-E.; Rebours, B.; Toulhoat, P. E. H. *J. Phys. Chem. B* **2001**, *105*, 5121.
- Yourdshahyan, Y.; Ruberto, C.; Halvarsson, M.; Bengtsson, L.; Langer, V.; Lundqvist, B. I.; Rupp, S.; Rolander, U. *J. Am. Ceram. Soc.* **1999**, *82*, 1365.
- Perdew, J. P.; Chevary, J. A.; Vosko, S. H.; Jackson, K. A.; Pederson, M. R.; Singh, D. J.; Fiolhais, C. *Phys. Rev. B* **1992**, *46*, 6671.
- Kresse, G.; Hafner, J. *Phys. Rev. B* **1993**, *48*, 13115.
- Kresse, G.; Furthmüller, J. *Comput. Mater. Sci.* **1996**, *6*, 15.
- Kresse, G.; Furthmüller, J. *Phys. Rev. B* **1996**, *54*, 11169.
- Blöchl, P. E. *Phys. Rev. B* **1994**, *50*, 17953.
- Kresse, G.; Joubert, D. *Phys. Rev. B* **1999**, *59*, 1758.
- Monkhorst, H. J.; Pack, J. D. *Phys. Rev. B* **1976**, *13*, 5188.
- $E_f = E_f^0(250) - (1/2)E_d(400)$. For the example of the initial reduction of the (1 × 1) structure at $\Theta = 1$ ML, the calculated energies are $E_f^0(400) = 5.18$ eV, $(1/2)E_d(400) = 3.15$ eV, $E_f^0(250) = 5.12$ eV, $(1/2)E_d(250) = 2.81$ eV.
- Herzberg, G. *Molecular Spectra and Molecular Structure. I. Spectra of Diatomic Molecules*, 2nd ed.; Robert E. Krieger Publishing Co. Inc.: Malabar, FL, 1989.
- Ollivier, B.; Retoux, R.; Lacorre, P.; Massiot, D.; Férey, G. *J. Mater. Chem.* **1997**, *7*, 1049.
- Ruberto, C.; Yourdshahyan, Y.; Lundqvist, B. I. *Phys. Rev. Lett.* **2002**, *88*, 226101.
- Ruberto, C.; Yourdshahyan, Y.; Lundqvist, B. I. *Phys. Rev. B* **2003**, *67*, 195412.
- Hyltdgaard, P.; Jacobson, N.; Ruberto, C.; Razaznejad, B.; Lundqvist, B. I. *Comput. Mater. Sci.* **2005**, *33*, 356.
- Tasker, P. W. *J. Phys. C* **1979**, *12*, 4977.
- Kresse, G.; Surnev, S.; Schoiswohl, J.; Netzer, F. P. *Surf. Sci.* **2004**, *555*, 118.
- Vyboishchikov, S. F.; Sauer, J. *J. Phys. Chem. A* **2000**, *104*, 10913.
- Calatayud, M.; Mguig, B.; Minot, C. *Surf. Sci.* **2003**, *526*, 297.
- Pykavy, M.; van Wüllen, C.; Sauer, J. *J. Chem. Phys.* **2004**, *120*, 4207.
- Chen, K.; Khodakov, A.; Yang, J.; Bell, A. T.; Iglesia, E. *J. Catal.* **1999**, *186*, 325.

- (47) Chen, K.; Iglesia, E.; Bell, A. T. *J. Catal.* **2000**, *192*, 197.
- (48) Ganduglia-Pirovano, M. V.; Sauer, J. *Phys. Rev. B* **2004**, *70*, 045422.
- (49) Ganduglia-Pirovano, M. V.; Sauer, J. *J. Phys. Chem. B* **2005**, *109*, 374.
- (50) Argyle, M. D.; Chen, K.; Bell, A. T.; Iglesia, E. *J. Catal.* **2002**, *208*, 139.
- (51) *Materials Thermochemistry*, 6th ed.; Kubaschewski, O., Alcock, C. B., Spencer, P. J., Eds.; Pergamon Press: Oxford, 1993.
- (52) Dupuis, A.-C.; Haija, M. A.; Richter, B.; Kuhlenbeck, H.; Freund, H.-J. *Surf. Sci.* **2003**, *539*, 99.
- (53) Schoiswohl, J.; Sock, M.; Surnev, S.; Ramsey, M. G.; Netzer, F.; Kresse, G.; Andersen, J. N. *Surf. Sci.* **2004**, *555*, 101.
- (54) Brázdová, V.; Ganduglia-Pirovano, M. V.; Sauer, J. *J. Phys. Chem. B* **2005**, *109*, 394.
- (55) Magg, N.; Immaraporn, B.; Giorgi, J. B.; Schroeder, T.; Bäumer, M.; Döbler, J.; Wu, Z.; Kondratenko, E.; Cherian, M.; Baerns, M.; Stair, P. C.; Sauer, J.; Freund, H.-J. *J. Catal.* **2004**, *226*, 88.